Gilbert damping for magnetic multilayers with perpendicular magnetic anisotropy

Yi Liu,[1,2] Pengtao Yang,[1] and Paul J. Kelly[2]

[1]*The Center for Advanced Quantum Studies and Department of Physics, Beijing Normal University, Beijing 100875, China*

[2]*Faculty of Science and Technology and MESA+ Institute for Nanotechnology, University of Twente, P. O. Box 217, 7500 AE Enschede, The Netherlands*

(Received 14 October 2023; accepted 2 January 2024; published 17 January 2024)

A systematic, computational study of the Gilbert damping in Co|Ni, Co|Pd, and Co|Pt multilayers is carried out using first-principles scattering calculations. The damping we find shows little temperature dependence and agrees well with experimental findings only when the interface damping enhancement is taken into account. In the absence of this extrinsic enhancement, the intrinsic damping of bulklike Co|Ni multilayers increases linearly with increasing ratio of Ni to Co layers. Though spin-orbit coupling is the common origin of magnetocrystalline anisotropy and magnetization damping, the latter is not sensitive to the interface roughness that affects magnetic anisotropy strongly.

DOI: 10.1103/PhysRevB.109.014416

I. INTRODUCTION

The discovery in layered magnetic structures [1,2] of oscillatory exchange coupling, giant magnetoresistance (GMR), perpendicular magnetic anisotropy (PMA), large magnetooptical effects, and spin-current-induced magnetization excitation and reversal has revealed a wealth of new phenomena that open up numerous possibilities for applications [3–11]. The spin-transfer torque (STT) predicted by Slonczewski [12] and Berger [13] and subsequently confirmed by experiment [14–21] forms the basis for new forms of magnetic data storage [22] like magnetic random access memories [23,24] or magnetic racetrack memory [25], where magnetic bits are read using the GMR effect and written using the STT or spin-orbit torque [26,27] effects. In striving to increase the density of stored data and reduce the currents required to write them, an important step has been the introduction of materials with large PMA such as Co|Ni multilayers [28–30]. Device performances are determined by fundamental properties of these multilayers (MLs) such as their anisotropy energies [31], spin-flip diffusion lengths [32–34], and Gilbert damping frequencies λ that restrict the operating length and timescales. However, current experimental measurements with a variety of ML structures yield a wide spread of parameter values. For example, for Co|Ni MLs that are of great interest because of their large magnetizations and because their magnetic anisotropy energies can be tuned, values of the dimensionless damping parameter α [35] ranging from 0.01 to 0.04 have been reported [36–46]. To identify the origin of this spread, we will focus in this paper on evaluating α for a number of these and related magnetic multilayers.

The dynamics of a magnetization $\mathbf{M}$ in an effective field $\mathbf{H}_{\rm eff}$ is usually described using the phenomenological Landau-Lifshitz-Gilbert equation [47,48],

$$\frac{d\mathbf{m}}{dt} = -\gamma \mathbf{m} \times \mathbf{H}_{\rm eff} + \alpha \mathbf{m} \times \frac{d\mathbf{m}}{dt}, \tag{1}$$

where $M_{\rm s} = |\mathbf{M}|$ is the saturation magnetization, $\mathbf{m} = \mathbf{M}/M_s$ is a unit vector in the magnetization direction, and $\gamma = g\mu_B/\hbar$ is the gyromagnetic ratio expressed in terms of the Landé g factor and the Bohr magneton μ_B. The first term in (1) describes the precessional motion of the magnetization in the effective field $\mathbf{H}_{\rm eff}$ that includes the external applied field as well as the exchange field, anisotropy, and demagnetization fields. The second term describes the time decay of the magnetization precession, the "Gilbert damping" [47,48], and determines the relaxation rate. Once the main contributions to the damping had been mapped out qualitatively [49], efforts to determine the damping parameter quantitatively focused on evaluating the torque correlation model (TCM) [50] within the relaxation time approximation using electronic structures calculated within the framework of density functional theory [51,52]. As a function of temperature, the damping is experimentally found to behave nonmonotonically with a well-defined minimum value. Gilmore and coworkers [52] took advantage of this nonmonotonic behavior to compare the measured minimum values to minimum values they calculated as a function of the relaxation time. The good agreement allowed them to conclude that the TCM contained the essential elements contributing to magnetization damping. Barati *et al.* extended this methodology to layered systems using tight-binding electronic structures [53–55] but the lack of experimental temperature-dependent studies of the damping in MLs made a direct comparison of theory and experiment impossible.

Inspired by the success of the spin-pumping theory [56] in explaining the enhancement of the Gilbert damping observed for a finite layer of magnetic material sandwiched between nonmagnetic metals [57] or forming bilayers with nonmagnetic metals [58], Brataas *et al.* derived an expression for the Gilbert damping within scattering theory [59] which has been implemented for a scattering geometry using a linearized muffin tin orbital (LMTO) basis [60,61] and in a bulk form with the Korringa-Kohn-Rostoker multiple-scattering method [62,63]. Excellent quantitative agreement was found for the temperature dependence of α for the important $Fe_{20}Ni_{80}$ alloy, permalloy [64] when (i) corrections for spin pumping and

radiative contributions were made in the experiments [65] and (ii) thermal lattice and spin disorder were taken into account on the same footing as alloy disorder in the calculations [61]. The prediction of very low damping for iron-rich FeCo alloys [62,63] was subsequently confirmed by experiment [66].

In this paper, we use the LMTO implementation of scattering theory to study systematically the value of the Gilbert damping parameter α in Co|X MLs with X = Ni, Pd, and Pt. We find that the "intrinsic" ML damping (no buffer or capping layers) shows little temperature dependence for any of these systems. For the specific cases of $Co_1|Ni_2$ and $Co_1|Ni_5$, α does not depend strongly on interface mixing (roughness). The main factor that influences α is an increasing Ni concentration because Ni has a much larger damping than does Co [67,68].

The damping calculated for Co|Pd and Co|Pt agrees reasonably well with experimental values but for Co|Ni it varies over a much smaller range than observed in experiment. With the knowledge that damping in ferromagnetic films can be greatly enhanced by contact with normal metal layers [56–58], we study the damping of Co|Ni MLs in contact with Pt with and without Cu layers in between, as these nonmagnetic metals are widely used as buffer/capping layers in experiments. The value of α obtained for Co|Ni directly in contact with Pt can be one order of magnitude larger than the intrinsic ML value and depends on the thicknesses of both the Co|Ni and Pt layers. Even when Cu layers separate the Co|Ni MLs from the Pt layers, the damping is still enhanced by more than a factor of two.

The paper is organized as follows. In Sec. II, a brief summary of the scattering formulation of damping is given followed by some technical details of how the calculations are performed and how the Gilbert damping parameter and resistivity are determined in practice. In Sec. III A, we study the Gilbert damping of Co|Ni, Co|Pd, and Co|Pt MLs with layer stacking ratios of 1:2 and 1:5 and compare the calculated results with previously reported experimental values. To account for the discrepancy between the calculations and measurements, we examine the interface enhancement of the damping in Co|Ni MLs in contact with Pt, and with Cu between Pt and CoNi in Sec. III B. The intrinsic damping of Co|Ni MLs is further studied in Sec. III C with different layer stacking and interface mixing. Comparison with other work is made and some conclusions are drawn in Sec. IV.

II. THEORETICAL METHOD AND COMPUTATIONAL DETAILS

Formulations of magnetization damping based on the Kubo formalism [50,51,69–75] and in terms of scattering theory have been shown to be equivalent in the linear response regime [59]. In the scattering formalism, the Gilbert damping tensor $\widetilde{G}$ for a single domain ferromagnetic metal (FM) sandwiched between left and right leads of a nonmagnetic (NM) material, denoted NM|FM|NM, can be expressed as

$$\widetilde{G}_{ij}(\mathbf{m}) = \frac{\gamma^2\hbar}{4\pi}\mathrm{Re}\left\{\mathrm{Tr}\left[\frac{\partial S}{\partial m_i}\frac{\partial S^\dagger}{\partial m_j}\right]\right\}. \tag{2}$$

The scattering matrix $S \equiv \begin{pmatrix} r & t' \\ t & r' \end{pmatrix}$ is composed of reflection and transmission matrices for Bloch waves incident from the left (r and t) or right (r' and t') leads. When spin-orbit coupling (SOC) is included, S depends on the magnetization direction $\mathbf{m}$. The microscopic picture of magnetization damping implicit in the scattering formalism is that energy is transferred from the electronic spin degrees of freedom through disorder scattering and SOC to the orbital degrees of freedom that is rapidly lost in thermal reservoirs attached to the leads. The conductance of the system (G, not to be confused with the damping tensor) can be calculated within the Landauer-Büttiker formalism as $G = (e^2|h)\mathrm{Tr}\{tt^\dagger\}$.

To calculate the scattering matrix at the Fermi level [76,77], we use a "wave-function matching" scheme [78] implemented with tight-binding linearized muffin-tin orbitals (TB-LMTOs) [79,80] that has been extended to include SOC [60,61]. The electronic structure of the NM|FM|NM sandwich is first determined self-consistently using a surface Greens function method [81] with a minimal basis of TB-LMTOs in the atomic spheres approximation. In the present study of (111) oriented Co|X MLs (X = Ni, Pd, and Pt), we consider a ML consisting of close-packed Co and X planes stacked in an *ABCABC* ... sequence that is attached to matching (111) oriented fcc Cu leads. This corresponds to a current-perpendicular-to-the-plane (CPP) geometry. Since the experimental lattice constants of bulk Co and Ni are quite similar, we calculate the Co|Ni lattice constants using Vegard's law and force the Cu leads to be matched in-plane [82]. For Co|Pd and Co|Pt MLs where Co is usually much thinner than Pd or Pt, we fix the (111) in-plane lattice constants of Co to match the values calculated for bulk fcc Pd and Pt and then determine layer separations by total energy minimization [83]. The in-plane lattice constants of the Cu leads are stretched to match the ML. The lead/scattering-region interface determines the interface resistance while the "bulk" properties we are interested in are not influenced by how the leads are modeled [84].

To calculate the Gilbert damping (and the electrical resistivity) there must be disorder. Because (i) the extrinsic disorder in the samples used in experimental studies is not known and (ii) most experiments are carried out at room temperature where thermal disorder can dominate scattering, it will be very convenient to introduce the following model of temperature-induced lattice and spin disorder [61,85,86]. Within the adiabatic approximation, "frozen" thermal lattice disorder is modelled by displacing atomic spheres rigidly and randomly from their ideal lattice positions in the scattering region subject to the Debye model [87] while "frozen" thermal spin disorder is modelled by tilting atomic magnetizations away from the quantization axis and rotating them randomly to reproduce the measured temperature-dependent magnetization [88]. Debye temperatures for single-crystal Ni (345 K), Pd (275 K), and Pt (225 K) taken from experiment [89] are used to describe the displacements of the same elements in the corresponding MLs. Because there is relatively little Co in these MLs and its Debye temperature (386 K) [89] does not differ greatly from the other Debye temperatures, the same displacements are, for simplicity, imposed on Co atoms. We use the magnetization measured for Co and Ni in the fitted form given in Ref. [90] to mimic spin disorder for the magnetic atoms. The spin disorder of the magnetization induced in Pd and Pt is treated like that of the Co atoms. The heroic nature

of these ad hoc approximations is justified by the subsequent finding that the damping is very insensitive to temperature, especially the amount of spin disorder.

To model the interface mixing that is presumed present in experimental MLs, we introduce interface disorder by randomly mixing atoms in adjacent atomic layers in the MLs [76,77]. For instance, for $Co_1|Ni_2 \equiv$ Ni|Co|Ni, $2n$ Co atoms from the Co layer are randomly distributed in the two adjacent Ni layers while the n substituted Ni atoms from each layer are distributed in the Co layer in exchange. The resulting layered structure is Ni|Co|Ni $\rightarrow$ $Ni_{1-x}Co_x|Co_{1-2x}Ni_{2x}|Ni_{1-x}Co_x$, or $Co_{1-2x}Ni_{2x}|(Ni_{1-x}Co_x)_2$. This mixing is performed only in the atomic layers forming the interface. For example, with interface-mixing $Co_1|Ni_5$ becomes $Ni_{1-x}Co_x|Co_{1-2x}Ni_{2x}|Ni_{1-x}Co_x|Ni_3$ with three Ni layers left unmixed.

Disorder in the scattering region is most conveniently modeled using large lateral supercells [76,77]. The two types of disorder described above are introduced into the scattering region using 5×5 lateral supercells perpendicular to the transport direction. The thickness of the scattering region is varied by adding complete ML periods. To sample the effect of modeling disorder in finite lateral supercells, a number of random configurations is generated for every thickness. The sample-to-sample spread is usually small and five configurations are found to be sufficient.

For a magnetic ML of thickness L, we write the total damping as $\widetilde{G}(L) = \widetilde{G}_{\rm if} + \widetilde{G}_b(L)$, where the interface contribution is $\widetilde{G}_{\rm if}$ and the bulk contribution is $\widetilde{G}_b(L) = \lambda V = \alpha\gamma M_s AL$, where A is the cross-sectional area. The dimensionless damping parameter α is then extracted from the slope of the total damping as shown in Fig. 1(b). We can decompose the total resistance of the system analogously as $R(L) = 1/G(L) = 1/G_{\rm sh} + 2R_{\rm if} + R_b(L)$, where $G_{\rm sh}$ is the Sharvin conductance of the ideal leads, $R_{\rm if}$ is the NM|FM interface resistance, and $R_b(L) = \rho L$ is the bulk contribution [61] and the resistivity ρ can be determined from the slope of the total resistance as shown in Fig. 1(a). The intercepts in both figures account for contributions from the leads and from the interfaces between the scattering region and the leads while the slopes corresponding to α and ρ are only determined by the properties of the bulklike multilayer in the scattering region and are independent of the choice of leads [84].

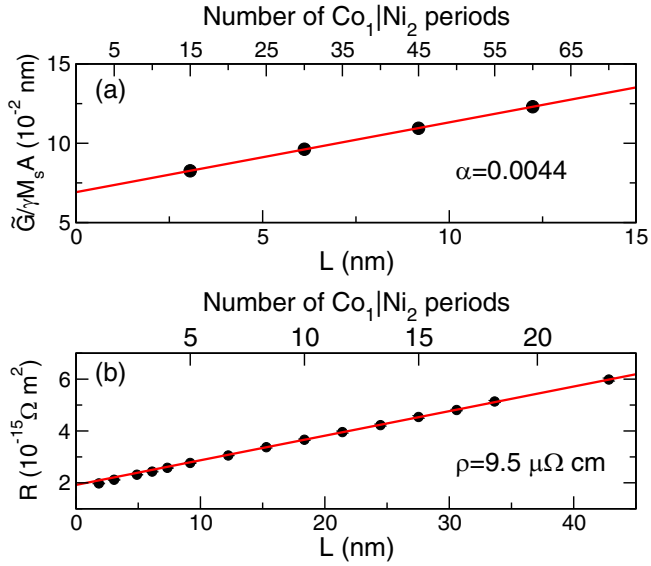

FIG. 1. Total damping (a) and resistance (b) calculated as a function of the thickness L for multiple $Co_1|Ni_2$ magnetic multilayers using Cu leads and including thermal disorder corresponding to the temperature $T = 300$ K. The solid lines in each panel show the best fit to extract the resistivity ρ (a) and the Gilbert damping parameter α (b). Each data point represents an average over 10 configurations of random thermal disorder and the standard deviation is smaller than the symbol size.

III. RESULTS

A. Gilbert damping of Co|X multilayers

We begin by examining the effect of thermal disorder on the damping of $Co_1|X_2$ and $Co_1|X_5$ MLs with X = Ni, Pd, and Pt where α is shown for the three temperatures $T = 200$, 300, and 400 K in Fig. 2. At best only a weak temperature dependence is found about room temperature ($T = 300$ K) irrespective of whether lattice and spin disorder (crosses) or only lattice disorder (empty squares) is included; spin fluctuations apparently make a negligible contribution to the magnetization damping at these temperatures. We have noted that weak temperature dependence can result from nonthermal electronic scattering mechanisms like the chemical disorder in substitutional $Ni_{80}Fe_{20}$ alloys [61] or from surface scattering in spatially confined single-layer Fe_3GeTe_2 [91]. In the present case, the interfaces between the Co and X layers scatter the conduction electrons strongly and do not depend on temperature.

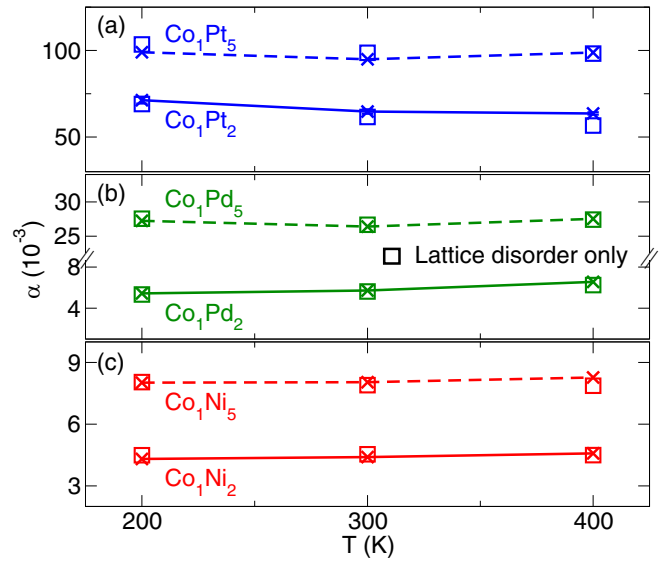

FIG. 2. Gilbert damping parameter α calculated for $Co_1|X_2$ (solid lines) and $Co_1|X_5$ (dashed lines) multilayers with X = Ni, Pd, and Pt as a function of the temperature with thermal lattice and spin disorder (crosses). Empty squares are results calculated including only thermal lattice disorder. All the errorbars are smaller than the symbol sizes.

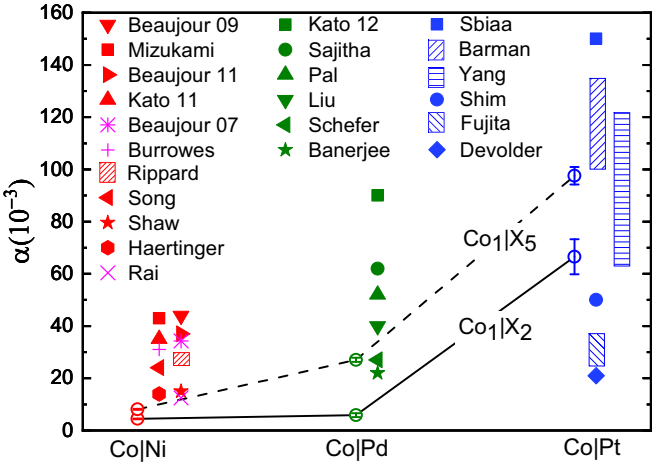

FIG. 3. Gilbert damping parameter α for $Co_1|X_2$ (solid lines) and $Co_1|X_5$ (dashed lines) multilayers for X = Ni, Pd, and Pt. The open circles show our calculated results where the error bars indicate the small variation with temperature we find. The other symbols [36–39,41–46,93–99,102,104] and bars [40,100,101,103] indicate measured values and value ranges, respectively. The multilayers studied in these experiments are briefly specified in Table I.

The values of α we calculate at room temperature are compared to a wide range of experimental values in Fig. 3 where the (modest) temperature variation found for $Co_1|X_2$ and $Co_1|X_5$ MLs in Fig. 2 is included as an error bar on the calculated values shown as open circles. α is seen to increase as the atomic number of X increases from Ni to Pd to Pt; and as the X concentration increases from $Co_1|X_2$ to $Co_1|X_5$. Values of α for $Co_1|Ni_2$, $Co_1|Ni_5$, and $Co_1|Pd_2$ are seen to be very similar. We can rationalize this in terms of the electronic structure of the Pd layers. In $Co_1|Pd_2$, the Pd layers on either side of the Co layer are magnetized with moments of about 0.32 μ_B per Pd atom compared to Ni moments of 0.64 μ_B per Ni atom in $Co_1|Ni_2$. We expect the Pd moments in Co_1Pd_2 will precess with the Co moments and not contribute to the damping. When more Pd layers are added, the proximity-induced magnetization of these Pd atoms decreases rapidly with their separation from the Co layer. Compared to $Co_1|Pd_2$, the three Pd layers in $Co_1|Pd_5$ not directly in contact with Co behave like NM metals and behave as spin sinks while the corresponding three magnetic Ni layers in $Co_1|Ni_5$ do not. The larger atomic SOC of Pd (compared to that of Ni) leads to the damping of $Co_1|Pd_5$ being a factor of two larger.

The magnetization induced on Pt in Co|Pt MLs is very similar to that induced on Pd in Co|Pd MLs. However, the Pt SOC is substantially larger than that for Pd: The SOC parameters ξ_d for Ni ($3d$), Pd ($4d$), and Pt ($5d$) are respectively 8, 14, and 44 mRyd where the spin-orbit splitting is $(l+\frac{1}{2})\xi_l$ [92]. $Co_1|Pt_2$ has a value of α which is one order of magnitude larger than that of $Co_1|Ni_2$ and $Co|Pd_2$ because the spin-orbit interaction on Pt is larger than its exchange interaction. Additional Pt layers with smaller exchange interactions behave as spin sinks and give rise to increased damping.

Compared to values of α reported from experiment, we find reasonable agreement for Co|Pd [93–98] and Co|Pt [99–104] though clearly more work is needed to reduce the spread of values seen in experiment. For Co|Ni, however, the experimental values are systematically larger than ours. As seen in Figs. 2 and 3, the value of α we calculate for Co|Ni MLs ranges from 0.004 to 0.008, while experimental values vary from 0.01 to 0.04 at room temperature [36–46]. A closer look at these experiments shows that the samples usually contain layers of heavy NM metals like Ta [39,40,43], Pd [37,38,41], and Pt [36,42,46] as buffer or capping layers. In the case of Co|Pd, a couple of experimental values are much larger [93–95] than ours and some of them contained thick Ta buffer layers. Knowing that damping in ferromagnetic films can be greatly enhanced by contact with normal metal layers [56], in the following section we look for an explanation for the large discrepancies in this direction.

B. Interface-enhanced damping in Co|Ni

To understand the discrepancies between the calculated and measured values of α for Co|Ni MLs, we study the effect of a Pt buffer (or capping) layer on the damping of a Co|Ni ML by placing a layer of fcc Pt of thickness l in contact with a Co|Ni ML which we choose to be $Co_1|Ni_2$. Because of the large difference in lattice constants between Pt and Co or Ni, we construct two-dimensional "lateral" supercells that match in the atomic plane perpendicular to the transport direction as follows. The in-plane lattice constant of $Co_1|Ni_2$ is kept fixed at its equilibrium value. A lateral supercell consisting of 3×3 primitive unit cells of $Co_1|Ni_2$ matches quite well to $\sqrt{7}\times\sqrt{7}$ primitive unit cells of Pt. It is then only necessary to stretch the lattice constant of Pt by 2% of its experimental value to achieve matching. A thickness d of $Co_1|Ni_2$ layers is alternated with a thickness l of Pt to form a scattering configuration as Cu-lead|$Co_1Ni_2(d)$|$Pt(l)$|$Co_1Ni_2(d)$|$Pt(l)$|...|Cu-lead where the "|" notation for the layering of $Co_1|Ni_2$ has been suppressed for clarity. Pt layer potentials are not determined self-consistently so unlike the Co|Pt MLs in the previous section, magnetic moments are not induced on Pt by proximity to the Co|Ni ML. The total damping of the system is calculated with room temperature frozen thermal lattice disorder in $Co_1|Ni_2$ and Pt; spin disorder is not included since it was already shown to have a negligible effect. The results are shown in Fig. 4.

Compared to the "intrinsic" value of $\alpha = 0.0044$ we found that for a $Co_1|Ni_2$ ML, indicated by the horizontal dashed line, the values of α found for $Co_1|Ni_2$ in contact with Pt layers are increased by one order of magnitude when $Co_1|Ni_2$ is thin, $d \sim 2$ nm. α decreases with a $1/d$ dependence as d increases and approaches the intrinsic damping value when d tends to infinity, as shown in the inset to Fig. 4. This is indicative of an interface damping enhancement that has been experimentally observed in permalloy films in contact with normal metal layers such as Pt, Pd, Ta, and Cu [57,105,106], modelled theoretically using "spin pumping" theory [56] and reproduced in first-principles calculations [107]. When interface enhancement is included, the values of α calculated for $Co_1|Ni_2$ MLs fall in the same range as the experimental values.

For example, in the experiment of Ref. [42], a 4.8-nm-thick ML of Co_2Ni_4 was sandwiched between 2-nm-thick layers of Pt on either side. According to the results of the calculations

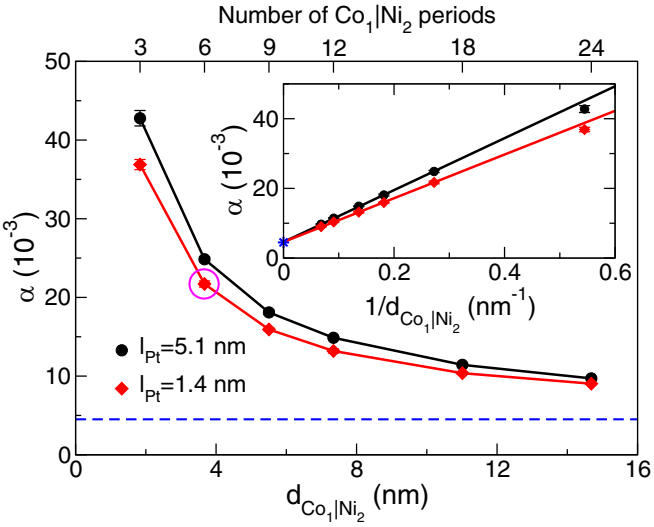

FIG. 4. Gilbert damping parameter α calculated as a function of d for a thickness d (nm) of $Co_1|Ni_2$ in contact with a thickness l of Pt, $Co_1Ni_2(d)|Pt(l)$. Two values of l are considered: $l = 5.1$ nm (black circles) and $l = 1.4$ nm (red diamonds), corresponding to 22 and 6 atomic layers, respectively. Thermal lattice disorder corresponding to $T = 300$ K is used. The horizontal dashed blue line indicates the damping we calculate for "bulk" $Co_1|Ni_2$. In the inset, α is replotted as a function of $1|d$ and the common intercept for $l = 5.1$ nm and $l = 1.4$ nm at $1/d = 0$ marked by the blue star is the "intrinsic" $Co_1|Ni_2$ damping. A specific data point for $d = 3.7$ nm and $l = 1.4$ nm (six slabs of Co_1Ni_2 and 6 atomic Pt layers) referred to in Fig. 5 is circled here for convenience.

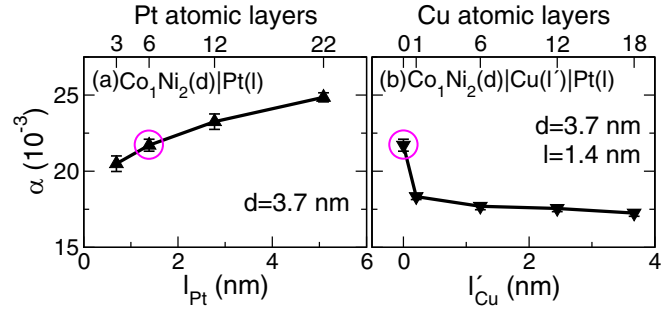

FIG. 5. Gilbert damping parameter α calculated for $Co_1|Ni_2$ multilayers (a) in direct contact with Pt layers: $Co_1Ni_2(d)Pt(l)$, as a function of the Pt layer thickness l with $d = 3.7$ nm (six periods of Co_1Ni_2) and (b) in contact with Cu layers adjacent to Pt layers: $Co_1Ni_2(d)|Cu(l')|Pt(l)$, as a function of the Cu layer thickness l' with $d = 3.7$ nm and $l = 1.4$ nm (six slabs of Co_1Ni_2 and six atomic Pt layers). The circled points are the same case.

shown in Fig. 4, we expect a damping enhancement of order 0.02, whereas the "intrinsic" $Co_1|Ni_2$ damping is only 0.0045 (dashed line in Fig. 4) and the measured value (red square in Fig. 3) is 0.043. Thus taking the damping enhancement by interface pumping into account indeed yields much better agreement; our value of $\alpha = 0.02$ falls in the experimental range in Fig. 4. The range of values reported by different experiments might be attributable to the sample-dependent interdiffusion of atoms between the CoNi MLs and the attached Pt film. Interface disorder enhances the (interface) spin memory loss significantly [108] and is expected to increase the total damping measured in experiment [107].

Changing the thickness l of the Pt layers changes the interface damping enhancement; see the difference between the black and red curves in Fig. 4. The result of calculating the damping as a function of the Pt layer thickness l for a fixed thickness $d = 3.7$ nm of $Co_1|Ni_2$, i.e., for $(Co_1|Ni_2)_6Pt(l)$ is shown in Fig. 5(a) where the damping enhancement is seen to increase monotonically with l. For $l = 5.1$ nm (22 atomic layers), α is more than 5 times larger than the "intrinsic" $Co_1|Ni_2$ value. This can also be explained using the spin pumping theory [56]. The precessing magnetization in $Co_1|Ni_2$ MLs pumps spin into the attached Pt layer where it decays via spin-flip disorder scattering. The thicker the Pt layers, the less spin current will flow back into $Co_1|Ni_2$ MLs, leading to a larger effective damping. The length scale on which this occurs in Pt is the spin-flip diffusion length $l_{Pt} \equiv l_{sf}^{Pt}$ which for Pt at room temperature is $l_{sf}^{Pt} \sim 5.3$ nm [34,84,86,107].

When damping is studied in magnetic MLs, a layer of Cu or Au is frequently inserted between the MLs and the Pt buffer or capping layer to determine the importance of having a direct interface between the ferromagnet and heavy metal with large SOC or of proximity-induced magnetism [36,39,109,110]. We can model such a situation by inserting a thin layer of Cu of thickness l' between a Co|Ni ML and Pt and study the effect of varying l' on the effective damping parameter for $(Co_1Ni_2)_6|Cu(l')|Pt_6$. The values of α we calculate are plotted in Fig. 5(b) where it can be seen that a single atomic layer of Cu inserted between $Co_1|Ni_2$ and Pt is enough to reduce the damping enhancement by 16%. This is perhaps surprising in view of our recent finding that the interface spin flipping (the spin memory loss) is, if anything, increased by insertion of a thin Cu layer at a FM|Pt interface [111]. Though the pumped spin current hardly decays in the Cu layer because of the very large value of $l_{Cu} \sim 500$ nm [111], the mixing conductance which governs the interface damping enhancement [56] can be quite different at the magnetic ML|Cu and ML|Pt interfaces. In Ref. [107], the mixing conductance at a Py|Cu interface was found to be much smaller than that at a Py|Pt interface, 0.48 versus 1.07, corresponding to a reduction in damping by 55% if Pt is replaced with Cu. We can expect a qualitatively similar situation here where inserting Cu between $Co_1|Ni_2$ and Pt can be expected to reduce the interface mixing conductance so that the damping enhancement is in turn reduced. When the thickness of the Cu layer is increased, the damping decreases slowly but is still much larger than the "bulk" $Co_1|Ni_2$ value.

In summary, our calculations suggest that the "intrinsic" Gilbert damping of Co|Ni MLs is much smaller than the reported experimental values. The damping can be greatly enhanced by placing Pt layers in either direct or indirect contact so that it varies in the same range as the measured values. Smaller enhancement is expected if not Pt but Pd or Ta is used as buffer/capping material [57], but it can still be tuned by adjusting the thicknesses of the Co|Ni MLs and normal metal layers. When reporting damping for magnetic MLs, it is essential to attribute this damping to the complete sample structure.

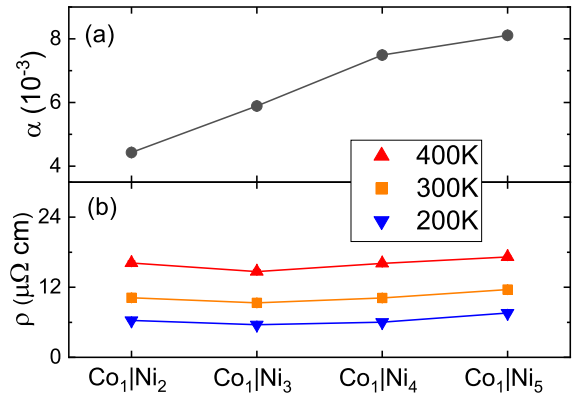

FIG. 6. Gilbert damping parameter α (a) and resistivity ρ (b) calculated for $Co_1|Ni_n$ multilayers with $n = 2, 3, 4, 5$ with frozen thermal lattice and spin disorder. The value variation with temperature in (a) is absorbed into error bars which are smaller than the size of the circles.

C. Damping in "bulk" Co|Ni multilayers

In the light of the above, we define an "intrinsic" damping for Co|Ni when there is no other normal metal layer in contact with CoNi. We already found in Fig. 2 for $Co_1|Ni_2$ and $Co_1|Ni_5$ that this intrinsic damping exhibited little temperature dependence. In Fig. 6(b) we see that the CPP resistivity ρ, in contrast and as expected, increases with increasing temperature. The intrinsic damping and resistivity calculated for the $Co_1|Ni_n$ ML series with $n = 2, 3, 4, 5$ including thermal lattice and spin disorder, shown in Fig. 6, confirm that the damping is independent of the temperature and its variance with temperature is much smaller than the size of the circles used in Fig. 6(a). This is because the intrinsic Ni damping is already saturated in this temperature range [67,68]. We note that the damping for this series of MLs increases almost linearly with increasing Ni concentration from $Co_1|Ni_2$ to $Co_1|Ni_5$. If we extrapolate back to $n = 0$, then we expect to find a damping for fcc Co of only $\alpha \sim 0.002$. In a previous study [85] we calculated a saturated bulk damping for Ni of about $\alpha \sim 0.02$ and $\alpha \sim 0.001$ for bulk hcp Co. Because of the dependence of the damping on structure, this means that the bulk hcp Co damping will not be reached on reducing the number of Ni layers in fcc Co|Ni MLs. Provided that the linear relation holds, of order $n \sim 15$ will be needed to observe the limit of bulk (fcc) Ni damping.

For MLs composed of similar sized atoms like Co and Ni, we expect substantial interface mixing in experimental samples [112–115]. To estimate the effect of such mixing on the Gilbert damping, we calculate α and ρ for $Co_1|Ni_2$ and $Co_1|Ni_5$ MLs with interface layers mixed to varying degrees. Results are shown in Fig. 7 for the corresponding $Co_{1-2x}Ni_{2x}|(Ni_{1-x}Co_x)_2$ and $Co_{1-2x}Ni_{2x}|(Ni_{1-x}Co_x)_2|Ni_3$ multilayers as a function of the mixing parameter x. Results for the corresponding homogeneous alloys are included for reference as dashed horizontal lines. Frozen thermal disorder is not included so the $x = 0$ limit for ordered structures is not well defined.

For $Co_1|Ni_2$, α does not depend on the interface mixing and takes values that are very close to what we calculate

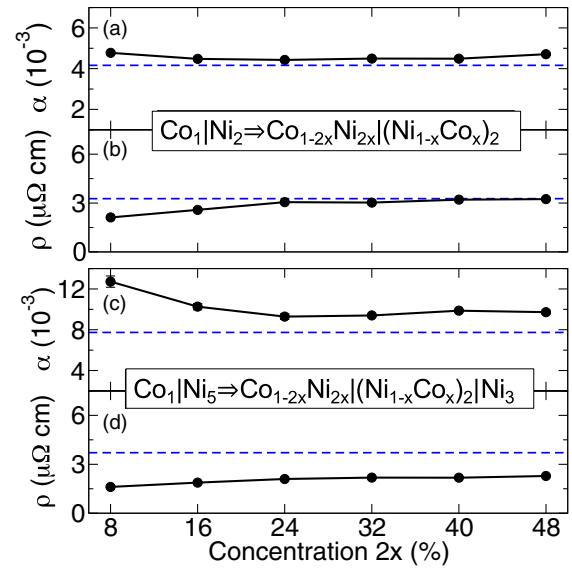

FIG. 7. Gilbert damping α [(a) and (c)] and resistivity ρ [(b) and (d)] as a function of the interface mixing parameter x for $Co_1|Ni_2$ and $Co_1|Ni_5$ multilayers, respectively. The effective structures are $Co_{1-2x}Ni_{2x}|(Ni_{1-x}Co_x)_2$ and $Co_{1-2x}Ni_{2x}|(Ni_{1-x}Co_x)_2|Ni_3$. The dashed lines indicate the corresponding results for homogeneous Co_1Ni_2 (upper panels) and Co_1Ni_5 (lower panels) alloys. All calculations are at zero temperature.

for the homogeneous alloy (which in turn is consistent with the result of a previous calculation [63]). ρ increases with increasing interface disorder and saturates to the value calculated for the homogeneous Co_1Ni_2 disordered alloy. For the $Co_1|Ni_5$ system, α decreases strongly at low values of x (from an ill-defined $x = 0$, $T = 0$ K limit) and then saturates to a value larger than that calculated for the homogeneous alloy while ρ saturates with increasing x to a value lower than that for the homogeneous alloy. The saturated values for both properties are different from the corresponding alloy results because $Co_{1-2x}Ni_{2x}|(Ni_{1-x}Co_x)_2|Ni_3$ still contains three "clean" Ni layers in the highly mixed limit. This leads to a larger value of α because ordered Ni is observed to show very strong so-called conductivity-like damping at low temperatures [62,67,68,85], and a lower value of ρ.

IV. DISCUSSION AND CONCLUSIONS

Insofar as the scattering formulation of magnetization damping has been shown to be identical to results obtained using the Kubo formalism [59], it is not surprising that our finding of a strong dependence of the damping in Co|X multilayers on the chemical identity of the material X is in agreement with the results of an earlier study based on a tight-binding implementation [53] of the TCM [50,74]. Comparison of our results with those of Barati *et al.* underline some of the advantages of our implementation. In particular, our introduction of thermal lattice and spin disorder [61,85,86] makes it possible to compare our results quantitatively with experiment as we do for Co|Ni, Co|Pd, and Co|Pt MLs in Fig. 3 without introducing phenomenological parameters like the relaxation time that figures prominently in the TCM. Our

first-principles scattering calculations allow us to model layered ML structures as well as chemical disorder realistically. The use of lateral supercells makes it possible to model interfaces between materials with very different lattice constants thus removing an important source of uncertainty on comparing with experiment.

We found the damping to be independent of temperature in the temperature range $200K < T < 400\,\mathrm{K}$ relevant for applications. Increasing the SOC from Ni to Pd to Pt leads to increased values of the Gilbert damping. Values of the damping parameter α calculated for Co|Ni MLs exhibit a much smaller range than reported experimental values. We suggest that the discrepancy results from the damping enhancement introduced by the heavy metal buffer/capping layers which are included in experimental samples. Calculations of the damping of Co|Ni MLs in contact with Pt show that α can be tuned by an order of magnitude and more. The enhancement remains and is still sizable even when Cu spacer layers are inserted between the Co|Ni MLs and the Pt buffer layers. This suggests that the complete sample structure should be specified when reporting damping values measured in magnetic MLs. For $Co_1|Ni_x$ MLs with $x = 2, 3, 4, 5$, the damping increases monotonically with increasing Ni concentration simply because Ni has a much larger damping than that of Co. We also showed that the interface mixing, which is usually present in experimental samples and weakens the magnetocrystalline anisotropy, does not influence the damping strongly.

ACKNOWLEDGMENTS

This work was financially supported by National Natural Science Foundation of China (Grants No. 12374101 and No. 11734004) as well as by the "Nederlandse Organisatie voor Wetenschappelijk Onderzoek" (NWO) through the research programme of the former "Stichting voor Fundamenteel Onderzoek der Materie," (NWO-I, formerly FOM) and through the use of supercomputer facilities of NWO "Exacte Wetenschappen" (Physical Sciences).

TABLE I. Summary of the multilayers used to determine the experimental values of the Gilbert damping in $Co(d_{Co})|X(d_X)$ ML systems (X=Ni, Pd, Pt) shown in Fig. 3. The layer thickness d_{Co} and d_X are given in Å units for Co and X, respectively.

Multilayer	d_{Co}	d_X	α	Reference
	1.4	8	0.044	Beaujour09 [37]
	1.4	8	0.037	Beaujour11 [41]
	2	4	0.0343	Beaujour07 [36]
	4	8	0.043	Mizukami [42]
	2.3	5.7		
Co|Ni	2.85	7.15	0.035	Kato11 [43]
	1.5	6	0.032	Burrowes [38]
	2	4	0.025–0.03	Rippard [40]
	3	7	0.024	Song [44]
	2	4	0.015	Shaw [39]
	1.5	7	0.014	Haertinger [45]
	2	6	0.0125	Rai [46]
	5.5	10	0.09	Kato12 [93]
	3	7	0.062	Sagitha [94]
Co|Pd	10	9	0.052	Pal [95]
	5	9	0.04	Liu [96]
	1.9	4	0.026	Schefer [97]
	5	10	0.022	Banerjee [98]
	3	8	0.15	Sbiaa [99]
	4	8	0.1–0.135	Barman [100]
Co|Pt	6	5–15	0.063–0.122	Yang [101]
	6.2	7.7	0.05	Shim [102]
	10–87	14	0.023–0.037	Fujita [103]
	5	3	0.021	Devolder [104]

APPENDIX: EXPERIMENTAL RESULTS

Values of the damping parameter α derived from different experiments for the multilayers shown in Fig. 3 are listed in Table I with details of the layer thicknesses of the samples studied.

[1] *Ultrathin Magnetic Structures I–IV*, edited by J. A. C. Bland and B. Heinrich (Springer-Verlag, Berlin, 1994-2005).

[2] S. Maekawa, S. O. Valenzuela, E. Saitoh, and T. Kimura, in *Spin Current*, 2nd ed., Semiconductor Science and Technology (Oxford University Press, Oxford, UK, 2017), Vol. 17.

[3] O. Boulle, J. Kimling, P. Warnicke, M. Kläui, U. Rüdiger, G. Malinowski, H. J. M. Swagten, B. Koopmans, C. Ulysse, and G. Faini, Nonadiabatic spin transfer torque in high anisotropy magnetic Nanowires with narrow domain walls, Phys. Rev. Lett. **101**, 216601 (2008).

[4] A. Hrabec, N. A. Porter, A. Wells, M. J. Benitez, G. Burnell, S. McVitie, D. McGrouther, T. A. Moore, and C. H. Marrows, Measuring and tailoring the Dzyaloshinskii-Moriya interaction in perpendicularly magnetized thin films, Phys. Rev. B **90**, 020402(R) (2014).

[5] S. Chung, S. M. Mohseni, S. R. Sani, E. Iacocca, R. K. Dumas, T. N. A. Nguyen, Y. Pogoryelov, P. K. Muduli, A. Eklund, M. Hoefer, and J. Åkerman, Spin transfer torque generated magnetic droplet solitons (invited), J. Appl. Phys. **115**, 172612 (2014).

[6] D. Backes, F. Macià, S. Bonetti, R. Kukreja, H. Ohldag, and A. D. Kent, Direct observation of a localized magnetic soliton in a spin-transfer nanocontact, Phys. Rev. Lett. **115**, 127205 (2015).

[7] A. Soumyanarayanan, M. Raju, A. L. G. Oyarce, A. K. C. Tan, M.-Y. Im, A. P. Petrović, P. Ho, K. H. Khoo, M. Tran, C. K. Gan, F. Ernult, and C. Panagopoulos, Tunable room-temperature magnetic skyrmions in Ir/Fe/Co/Pt multilayers, Nat. Mater. **16**, 898 (2017).

[8] C. Safranski, J. Z. Sun, J.-W. Xu, and A. D. Kent, Planar Hall driven torque in a ferromagnet/nonmagnet/ferromagnet system, Phys. Rev. Lett. **124**, 197204 (2020).

[9] B. Cui, D. Yu, Z. Shao, Y. Liu, H. Wu, P. Nan, Z. Zhu, C. Wu, T. Guo, P. Chen, H.-A. Zhou, L. Xi, W. Jiang, H. Wang,

S. Liang, H. Du, K. L. Wnag, W. Wang, K. Wu, X. Han *et al.*, Néel-type elliptical skyrmions in a laterally asymmetric magnetic multilayer, Adv. Mater. **33**, 2006924 (2021).

[10] N. Figueiredo-Prestes, S. Krishnia, S. Collin, Y. Roussigné, M. Belmeguenai, S. M. Chérif, J. Zarpellon, D. H. Mosca, H. Jaffrès, L. Vila, N. Reyren, and J.-M. George, Magnetization switching and deterministic nucleation in Co/Ni multilayered disks induced by spin-orbit torques, Appl. Phys. Lett. **119**, 032410 (2021).

[11] X. Chen, E. Chue, J. F. Kong, H. R. Tan, H. K. Tan, and A. Soumyanarayanan, Thermal evolution of skyrmion formation mechanism in chiral multilayer film, Phys. Rev. Appl. **17**, 044039 (2022).

[12] J. C. Slonczewski, Current-driven excitation of magnetic multilayers, J. Magn. Magn. Mater. **159**, L1 (1996).

[13] L. Berger, Emission of spin waves by a magnetic multilayer traversed by a current, Phys. Rev. B **54**, 9353 (1996).

[14] M. Tsoi, A. G. M. Jansen, J. Bass, W.-C. Chiang, M. Seck, V. Tsoi, and P. Wyder, Excitation of a magnetic multilayer by an electric current, Phys. Rev. Lett. **80**, 4281 (1998).

[15] J. Z. Sun, Current-driven magnetic switching in manganite trilayer junctions, J. Magn. Magn. Mater. **202**, 157 (1999).

[16] J.-E. Wegrowe, D. Kelly, Y. Jaccard, Ph. Guittienne, and J. Ph. Ansermet, Current-induced magnetization reversal in magnetic nanowires, Europhys. Lett. **45**, 626 (1999).

[17] E. B. Myers, D. C. Ralph, J. A. Katine, R. N. Louie, and R. A. Buhrman, Current-induced switching of domains in magnetic multilayer devices, Science **285**, 867 (1999).

[18] J. A. Katine, F. J. Albert, R. A. Buhrman, E. B. Myers, and D. C. Ralph, Current-driven magnetization reversal and spin-wave excitations in Co/Cu/Co pillars, Phys. Rev. Lett. **84**, 3149 (2000).

[19] M. Tsoi, A. G. M. Jansen, J. Bass, W.-C. Chiang, V. Tsoi, and P. Wyder, Generation and detection of phase-coherent current-driven magnons in magnetic multilayers, Nature (London) **406**, 46 (2000).

[20] J. Grollier, A. H. V. Cros, J. M. George, H. Jaffrès, A. Fert, G. Faini, J. B. Youssef, and H. Legall, Spin-polarized current induced switching in Co/Cu/Co pillars, Appl. Phys. Lett. **78**, 3663 (2001).

[21] S. I. Kiselev, J. C. Sankey, I. N. Krivorotov, N. C. Emley, R. J. Schoelkopf, R. A. Buhrman, and D. C. Ralph, Microwave oscillations of a nanomagnet driven by a spin-polarized current, Nature (London) **425**, 380 (2003).

[22] S. Bhatti, R. Sbiaa, A. Hirohata, H. Ohno, S. Fukami, and S. N. Piramanayagam, Spintronics based random access memory: A review, Mater. Today **20**, 530 (2017).

[23] J. Åkerman, Toward a universal memory, Science **308**, 508 (2005).

[24] M. H. Kryder and C. S. Kim, After hard drives—What comes next? IEEE Trans. Magn. **45**, 3406 (2009).

[25] S. S. P. Parkin, M. Hayashi, and L. Thomas, Magnetic domain-wall racetrack memory, Science **320**, 190 (2008).

[26] A. Brataas and K. M. D. Hals, Spin-orbit torques in action, Nat. Nanotechnol. **9**, 86 (2014).

[27] A. Manchon, J. Železný, I. M. Miron, T. Jungwirth, J. Sinova, A. Thiaville, K. Garello, and P. Gambardella, Current-induced spin-orbit torques in ferromagnetic and antiferromagnetic systems, Rev. Mod. Phys. **91**, 035004 (2019).

[28] S. Mangin, D. Ravelosona, J. A. Katine, M. J. Carey, B. D. Terris, and E. E. Fullerton, Current-induced magnetization reversal in nanopillars with perpendicular anisotropy, Nat. Mater. **5**, 210 (2006).

[29] D. Houssameddine, U. Ebels, B. Delaët, B. Rodmacq, I. Firastrau, F. Ponthenier, M. Brunet, C. Thirion, J.-P. Michel, L. Prejbeanu-Buda, M.-C. Cyrille, O. Redon, and B. Dieny, Spin-torque oscillator using a perpendicular polarizer and a planar free layer, Nat. Mater. **6**, 447 (2007).

[30] S. Mangin, Y. Henry, D. Ravelosona, J. A. Katine, and E. E. Fullerton, Reducing the critical current for spin-transfer switching of perpendicularly magnetizaed nanomagnets, Appl. Phys. Lett. **94**, 012502 (2009).

[31] M. T. Johnson, P. J. H. Bloemen, F. J. A. den Broeder, and J. J. de Vries, Magnetic anisotropy in metallic multilayers, Rep. Prog. Phys. **59**, 1409 (1996).

[32] J. Bass and W. P. Pratt, Jr., Spin-diffusion lengths in metals and alloys, and spin-flipping at metal/metal interfaces: An experimentalist's critical review, J. Phys.: Condens. Matter **19**, 183201 (2007).

[33] J. Sinova, S. O. Valenzuela, J. Wunderlich, C. H. Back, and T. Jungwirth, Spin Hall effects, Rev. Mod. Phys. **87**, 1213 (2015).

[34] R. S. Nair, E. Barati, K. Gupta, Z. Yuan, and P. J. Kelly, Spin-flip diffusion length in $5d$ transition metal elements: A first-principles benchmark, Phys. Rev. Lett. **126**, 196601 (2021).

[35] α and λ are related as $\lambda = \gamma\alpha M_S$, where γ is the gyromagnetic ratio and M_s is the saturation magnetization density [85].

[36] J.-M. L. Beaujour, W. Chen, K. Krycka, C.-C. Kao, J. Z. Sun, and A. D. Ken, Ferromagnetic resonance study of sputtered Co|Ni multilayers, Eur. Phys. J. B **59**, 475 (2007).

[37] J.-M. Beaujour, D. Ravelosona, I. Tudosa, E. E. Fullerton, and A. D. Kent, Ferromagnetic resonance linewidth in ultrathin films with perpendicular magnetic anisotropy, Phys. Rev. B **80**, 180415(R) (2009).

[38] C. Burrowes, A. P. Mihai, D. Ravelosona, J.-V. Kim, C. Chappert, L. Vila, A. Marty, Y. Samson, F. Garcia-Sanchez, L. D. Buda-Prejbeanu, I. Tudosa, E. E. Fullerton, and J.-P. Attané, Non-adiabatic spin-torques in narrow magnetic domain walls, Nat. Phys. **6**, 17 (2010).

[39] J. M. Shaw, H. T. Nembach, and T. J. Silva, Roughness induced magnetic inhomogeneity in Co/Ni multilayers: Ferromagnetic resonance and switching properties in nanostructures, J. Appl. Phys. **108**, 093922 (2010).

[40] W. H. Rippard, A. M. Deac, M. R. Pufall, J. M. Shaw, M. W. Keller, S. E. Russek, G. E. W. Bauer, and C. Serpico, Spin-transfer dynamics in spin valves with out-of-plane magnetized CoNi free layers, Phys. Rev. B **81**, 014426 (2010).

[41] J.-M. Beaujour, A. D. Kent, D. Ravelosona, I. Tudosa, and E. E. Fullerton, Ferromagnetic resonance study of Co/Pd/Co/Ni multilayers with perpendicular anisotropy irradiated with helium ions, J. Appl. Phys. **109**, 033917 (2011).

[42] S. Mizukami, X. Zhang, T. Kubota, H. Naganuma, M. Oogane, Y. Ando, and T. Miyazaki, Gilbert damping in Ni/Co multilayer films exhibiting large perpendicular anisotropy, Appl. Phys. Express **4**, 013005 (2011).

[43] T. Kato, Y. Matsumoto, S. Okamoto, N. Kikuchi, O. Kitakami, N. Nishizawa, S. Tsunashima, and S. Iwata, Time-resolved magnetization dynamics and damping constant of sputtered Co/Ni multilayers, IEEE Trans. Magn. **47**, 3036 (2011).

[44] H.-S. Song, K.-D. Lee, J.-W. Sohn, S.-H. Yang, S. S. P. Parkin, C.-Y. You, and S.-C. Shin, Observation of the intrinsic Gilbert damping constant in Co/Ni multilayers independent of the stack number with perpendicular anisotropy, Appl. Phys. Lett. **102**, 102401 (2013).

[45] M. Haertinger, C. H. Back, S. H. Yang, S. S. P. Parkin, and G. Woltersdorf, Properties of Ni/Co multilayers as a function of the number of multilayer repetitions, J. Phys. D: Appl. Phys. **46**, 175001 (2013).

[46] A. Rai, A. Sapkota, A. Pokhrel, M. Li, M. D. Graef, C. Mewes, V. Sokalski, and T. Mewes, Higher-order perpendicular magnetic anisotropy and interfacial damping of Co/Ni multilayers, Phys. Rev. B **102**, 174421 (2020).

[47] T. L. Gilbert, A Lagrangian formulation of the gyromagnetic equation of the magnetization field, Phys. Rev. **100**, 1243 (1955).

[48] T. L. Gilbert, A phenomenological theory of damping in ferromagnetic materials, IEEE Trans. Magn. **40**, 3443 (2004).

[49] B. Heinrich, Spin relaxation in magnetic metallic layers and multilayers, in *Ultrathin Magnetic Structures III*, edited by J. A. C. Bland and B. Heinrich (Springer, New York, 2005), pp. 143–210.

[50] V. Kamberský, On ferromagnetic resonance damping in metals, Czech. J. Phys. **26**, 1366 (1976).

[51] J. Kuneš and V. Kamberský, First-principles investigation of the damping of fast magnetization precession in ferromagnetic 3d metals, Phys. Rev. B **65**, 212411 (2002); **68**, 019901(E) (2003).

[52] K. Gilmore, Y. U. Idzerda, and M. D. Stiles, Identification of the dominant precession-damping mechanism in Fe, Co, and Ni by first-principles calculations, Phys. Rev. Lett. **99**, 027204 (2007); Spin-orbit precession damping in transition metal ferromagnets, J. Appl. Phys. **103**, 07D303 (2008).

[53] E. Barati, M. Cinal, D. M. Edwards, and A. Umerski, Gilbert damping in magnetic layered systems, Phys. Rev. B **90**, 014420 (2014).

[54] E. Barati and M. Cinal, Quantum mechanism of nonlocal Gilbert damping in magnetic trilayers, Phys. Rev. B **91**, 214435 (2015).

[55] E. Barati and M. Cinal, Gilbert damping in binary magnetic multilayers, Phys. Rev. B **95**, 134440 (2017).

[56] Y. Tserkovnyak, A. Brataas, and G. E. W. Bauer, Enhanced Gilbert damping in thin ferromagnetic films, Phys. Rev. Lett. **88**, 117601 (2002); Spin pumping and magnetization dynamics in metallic multilayers, Phys. Rev. B **66**, 224403 (2002).

[57] S. Mizukami, Y. Ando, and T. Miyazaki, The study on ferromagnetic resonance linewidth for NM/80NiFe/NM (NM = Cu, Ta, Pd and Pt) films, Jpn. J. Appl. Phys. **40**, 580 (2001); Ferromagnetic resonance linewidth for NM/80NiFe/NM films (NM=Cu, Ta, Pd and Pt), J. Magn. Magn. Mater. **226-230**, 1640 (2001).

[58] R. Urban, G. Woltersdorf, and B. Heinrich, Gilbert damping in single and multilayer ultrathin films: Role of interfaces in nonlocal spin dynamics, Phys. Rev. Lett. **87**, 217204 (2001).

[59] A. Brataas, Y. Tserkovnyak, and G. E. W. Bauer, Scattering theory of Gilbert damping, Phys. Rev. Lett. **101**, 037207 (2008); Magnetization dissipation in ferromagnets from scattering theory, Phys. Rev. B **84**, 054416 (2011).

[60] A. A. Starikov, P. J. Kelly, A. Brataas, Y. Tserkovnyak, and G. E. W. Bauer, Unified first-principles study of Gilbert damping, spin-flip diffusion and resistivity in transition metal alloys, Phys. Rev. Lett. **105**, 236601 (2010).

[61] A. A. Starikov, Y. Liu, Z. Yuan, and P. J. Kelly, Calculating the transport properties of magnetic materials from first-principles including thermal and alloy disorder, non-collinearity and spin-orbit coupling, Phys. Rev. B **97**, 214415 (2018).

[62] H. Ebert, S. Mankovsky, D. Ködderitzsch, and P. J. Kelly, *Ab Initio* calculation of the Gilbert damping parameter via linear response formalism, Phys. Rev. Lett. **107**, 066603 (2011).

[63] S. Mankovsky, D. Ködderitzsch, G. Woltersdorf, and H. Ebert, First-principles calculation of the Gilbert damping parameter via the linear response formalism with application to magnetic transition metals and alloys, Phys. Rev. B **87**, 014430 (2013).

[64] Y. Zhao, Q. Song, S.-H. Yang, T. Su, W. Yuan, S. S. P. Parkin, J. Shi, and W. Han, Experimental investigation of temperature-dependent Gilbert damping in permalloy thin films, Sci. Rep. **6**, 22890 (2016).

[65] M. A. W. Schoen, J. Lucassen, H. T. Nembach, T. J. Silva, B. Koopmans, C. H. Back, and J. M. Shaw, Magnetic properties of ultrathin 3*d* transition-metal binary alloys. I. Spin and orbital moments, anisotropy, and confirmation of Slater-Pauling behavior, Phys. Rev. B **95**, 134410 (2017).

[66] M. A.W. Schoen, D. Thonig, M. L. Schneider, T. J. Silva, H. T. Nembach, O. Eriksson, O. Karis, and J. M. Shaw, Ultra-low magnetic damping of a metallic ferromagnet, Nat. Phys. **12**, 839 (2016).

[67] S. M. Bhagat and P. Lubitz, Temperature variation of ferromagnetic relaxation in the 3*d* transition metals, Phys. Rev. B **10**, 179 (1974).

[68] B. Heinrich, D. J. Meredith, and J. F. Cochran, Wave number and temperature-dependent Landau-Lifshitz damping in nickel, J. Appl. Phys. **50**, 7726 (1979).

[69] B. Heinrich, D. Fraitová, and V. Kamberský, The influence of s-d exchange on relaxation of magnons in metals, Physica Status Solidi (b) **23**, 501 (1967).

[70] V. Kamberský, On the Landau-Lifshitz relaxation in ferromagnetic metals, Can. J. Physica **48**, 2906 (1970).

[71] V. Korenman and R. E. Prange, Anomalous damping of spin waves in magnetic metals, Phys. Rev. B **6**, 2769 (1972).

[72] V. S. Lutovinov and M. Y. Reizer, Relaxation processes in ferromagnetic metals, Zh. Eksp. Teor. Fiz. **77**, 707 (1979) [Sov. Phys. JETP **50**, 355 (1979)].

[73] V. L. Safonov and H. N. Bertram, Impurity relaxation mechanism for dynamic magnetization reversal in a single domain grain, Phys. Rev. B **61**, R14893 (2000).

[74] V Kamberský, Spin-orbital Gilbert damping in common magnetic metals, Phys. Rev. B **76**, 134416 (2007).

[75] I. Garate, K. Gilmore, M. D. Stiles, and A. H. MacDonald, Nonadiabatic spin-transfer torque in real materials, Phys. Rev. B **79**, 104416 (2009).

[76] K. Xia, P. J. Kelly, G. E. W. Bauer, I. Turek, J. Kudrnovský, and V. Drchal, Interface resistance of disordered magnetic multilayers, Phys. Rev. B **63**, 064407 (2001).

[77] K. Xia, M. Zwierzycki, M. Talanana, P. J. Kelly, and G. E. W. Bauer, First-principles scattering matrices for spin-transport, Phys. Rev. B **73**, 064420 (2006).

[78] T. Ando, Quantum point contacts in magnetic fields, Phys. Rev. B **44**, 8017 (1991).

[79] O. K. Andersen, Linear methods in band theory, Phys. Rev. B **12**, 3060 (1975).

[80] O. K. Andersen, Z. Pawlowska, and O. Jepsen, Illustration of the linear-muffin-tin-orbital tight-binding representation: Compact orbitals and charge density in Si, Phys. Rev. B **34**, 5253 (1986).

[81] I. Turek, V. Drchal, J. Kudrnovský, M. Šob, and P. Weinberger, *Electronic Structure of Disordered Alloys, Surfaces and Interfaces* (Kluwer, Dordrecht, 1997).

[82] The experimental lattice constants for bulk fcc Ni and Cu are $a_{\mathrm{Ni}} = 3.524$ Å and $a_{\mathrm{Cu}} = 3.614$ Å, respectively. The experimental lattice constants for hcp Co are converted to an fcc structure, leading to $a_{\mathrm{Co}} = 3.549$ Å, subject to the constraint that the atomic volume is conserved.

[83] G. H. O. Daalderop, P. J. Kelly, and M. F. H. Schuurmans, First-principles calculation of the magnetic anisotropy energy of $(\mathrm{Co})_n/(\mathrm{X})_m$ multilayers, Phys. Rev. B **42**, 7270 (1990).

[84] R. J. H. Wesselink, K. Gupta, Z. Yuan, and P. J. Kelly, Calculating spin transport properties from first principles: Spin currents, Phys. Rev. B **99**, 144409 (2019).

[85] Y. Liu, A. A. Starikov, Z. Yuan, and P. J. Kelly, First-principles calculations of magnetization relaxation in pure Fe, Co, and Ni with frozen thermal lattice disorder, Phys. Rev. B **84**, 014412 (2011).

[86] Y. Liu, Z. Yuan, R. J. H. Wesselink, A. A. Starikov, M. van Schilfgaarde, and P. J. Kelly, Direct method for calculating temperature-dependent transport properties, Phys. Rev. B **91**, 220405(R) (2015).

[87] In Ref. [86] we determined static lattice disorder for the NM metals Cu, Pd, and Pt, from phonon spectra calculated from first principles. The same scattering calculations as are used in the present work yielded temperature dependent resistivities in good agreement with experiment.

[88] In Ref. [86] spin disorder was determined for Fe and permalloy ($\mathrm{Ni_{80}Fe_{20}}$) by calculating magnon spectra from first principles and populating them by analogy with our treatment of phonons. The resulting "frozen" lattice and spin disorder underestimated the decrease with temperature of the magnetization and the increase of the resistivity because of well-known and understood shortcomings of spin wave theory. When we adopted Gaussian spin disorder and chose the width so as to reproduce the temperature magnetization, the calculated resistivity and anisotropic magnetoresistance were in agreement with measured values. These examples justify the use of "frozen" lattice and spin disorder until discrepancies emerge in future experiments.

[89] C. Y. Ho, R. W. Powell, and P. E. Liley, Thermal conductivity of the elements, J. Phys. Chem. Ref. Data **1**, 279 (1972).

[90] M. D. Kuz'min, Shape of temperature dependence of spontaneous magnetization of ferromagnets: Quantitative analysis, Phys. Rev. Lett. **94**, 107204 (2005).

[91] P. Yang, R. Liu, Z. Yuan, and Y. Liu, Magnetic damping anisotropy in the two-dimensional van der Waals material $\mathrm{Fe_3GeTe_2}$ from first principles, Phys. Rev. B **106**, 134409 (2022).

[92] O. K. Andersen, O. Jepsen, and D. Glötzel, Canonical description of the band structures of metals, in *Highlights of Condensed Matter Theory*, International School of Physics 'Enrico Fermi', Varenna, Italy, edited by F. Bassani, F. Fumi, and M. P. Tosi (North-Holland, Amsterdam, 1985), pp. 59–176.

[93] T. Kato, Y. Matsumoto, S. Kashima, S. Okamoto, N. Kikuchi, S. Iwata, O. Kitakami, and S. Tsunashima, Perpendicular anisotropy and Gilbert damping in sputtered Co/Pd multilayers, IEEE Trans. Magn. **48**, 3288 (2012).

[94] E. P. Sajitha, J. Walowski, D. Watanabe, S. Mizukami, F. Wu, H. Naganuma, M. Oogane, Y. Ando, and T. Miyazaki, Magnetisation dynamics in CoFeB buffered perpendicularly magnetized Co/Pd multilayer, IEEE Trans. Magn. **46**, 2056 (2010).

[95] S. Pal, B. Rana, O. Hellwig, T. Thomson, and A. Barman, Tunable magnonic frequency and damping in $[\mathrm{Co/Pd}]_8$ multilayers with variable Co layer thickness, Appl. Phys. Lett. **98**, 082501 (2011).

[96] Z. Liu, R. Brandt, O. Hellwig, S. Florez, T. Thomson, B. Terris, and H. Schmidt, Thickness dependent magnetization dynamics of perpendicular anisotropy Co/Pd multilayer films, J. Magn. Magn. Mater. **323**, 1623 (2011).

[97] T. A. Schefer, D. L. Cortie, and M. Kostylev, The effect of hydrogen gas on $\mathrm{Pd/[Co/Pd]_{30}/Pd}$ multilayer thin films, J. Magn. Magn. Mater. **551**, 169184 (2022).

[98] C. Banerjee, S. Pal, M. Ahlberg, T. N. Anh Nguyen, J. Åkerman, and A. Barman, All-optical study of tunable ultrafast spin dynamics in [Co/Pd]/NiFe systems: The role of spin-twist structure on Gilbert damping, RSC Adv. **6**, 80168 (2016).

[99] R. Sbiaa, J. M. Shaw, H. T. Nembach, M. Al Bahri, M. Ranjbar, J. Åkerman, and S. N. Piramanayagam, Ferromagnetic resonance measurements of (Co/Ni/Co/Pt) multilayers with perpendicular magnetic anisotropy, J. Phys. D: Appl. Phys. **49**, 425002 (2016).

[100] A. Barman, S. Wang, O. Hellwig, A. Berger, E. E. Fullerton, and H. Schmidt, Ultrafast magnetization dynamics in high perpendicular anisotropy $[\mathrm{Co/Pt}]_n$ multilayers, J. Appl. Phys. **101**, 09D102 (2007).

[101] X.-Y. Yang, W. Li, J.-Q. Yan, Y.-J. Bian, Y.-Y. Zhang, S.-T. Lou, Z.-Z. Zhang, X. L. Zhang, and Q. Y. Jin, Magnetic damping in perpendicular $[\mathrm{Pt/Co}]_3$/MnIr multilayers, J. Magn. Magn. Mater. **487**, 165286 (2019).

[102] J.-H. Shim, A. A. Syed, Y. Shin, J.-W. Kim, H.-G. Piao, S.-H. Lee, K. M. Lee, J.-R. Jeong, D.-H. Kim, and D. E. Kim, Ultrafast dynamics of exchange stiffness in Co/Pt multilayer, Commun. Phys. **3**, 74 (2020).

[103] N. Fujita, N. Inaba, F. Kirino, S. Igarashi, K. Koike, and H. Kato, Damping constant of Co/Pt multilayer thin-film media, J. Magn. Magn. Mater. **320**, 3019 (2008).

[104] T. Devolder, S. Couet, J. Swerts, and G. S. Kar, Gilbert damping of high anisotropy Co/Pt multilayers, J. Phys. D: Appl. Phys. **51**, 135002 (2018).

[105] S. Mizukami, Y. Ando, and T. Miyazaki, Magnetic relaxation of normal-metal (NM)/80NiFe/NM films, J. Magn. Magn. Mater. **239**, 42 (2002).

[106] S. Azzawi, A. Ganguly, M. Tokaç, R. M. Rowan-Robinson, J. Sinha, A. T. Hindmarch, A. Barman, and D. Atkinson, Evolution of damping in ferromagnetic/nonmagnetic thin film bilayers as a function of nonmagnetic layer thickness, Phys. Rev. B **93**, 054402 (2016).

[107] Y. Liu, Z. Yuan, R. J. H. Wesselink, A. A. Starikov, and P. J. Kelly, Interface enhancement of Gilbert damp-

ing from first principles, Phys. Rev. Lett. **113**, 207202 (2014).

[108] K. Gupta, R. J. H. Wesselink, R. Liu, Z. Yuan, and P. J. Kelly, Disorder dependence of interface spin memory loss, Phys. Rev. Lett. **124**, 087702 (2020).

[109] C. Swindells, H. Głowiński, Y. Choi, D. Haskel, P. P. Michałowski, T. Hase, F. Stobiecki, P. Kuświk, and D. Atkinson, Magnetic damping in ferromagnetic/heavy-metal systems: The role of interfaces and the relation to proximity-induced magnetism, Phys. Rev. B **105**, 094433 (2022).

[110] C. Swindells, H. Głowiński, Y. Choi, D. Haskel, P. P. Michałowski, T. Hase, P. Kuświk, and D. Atkinson, Proximity-induced magnetism and the enhancement of damping in ferromagnetic/heavy metal systems, Appl. Phys. Lett. **119**, 152401 (2021).

[111] R. Liu, K. Gupta, Z. Yuan, and P. J. Kelly, Calculating the spin memory loss at Cu|metal interfaces from first principles, Phys. Rev. B **106**, 014401 (2022).

[112] F. J. Lamelas, C. H. Lee, H. He, W. Vavra, and R. Clarke, Coherent fcc stacking in epitaxial Co/Cu superlattices, Phys. Rev. B **40**, 5837 (1989).

[113] H. A. M. de Gronckel, K. Kopinga, W. J. M. de Jonge, P. Panissod, J. P. Schillé, and F. J. A. den Broeder, Nanostructure of Co/Cu multilayers, Phys. Rev. B **44**, 9100 (1991).

[114] C. Mény, P. Panissod, and R. Loloee, Structural study of cobalt-copper multilayers by NMR, Phys. Rev. B **45**, 12269 (1992).

[115] C. Kapusta, P. Fischer, and G. Schütz, Magnetic x-ray absorption spectroscopy, J. Alloys Compd. **286**, 37 (1999).